Additive Manufacturing 30 (2019) 100894

Contents lists available at ScienceDirect

Additive Manufacturing

journal homepage: www.elsevier.com/locate/addma

Review

Additive manufacturing in construction: A review on processes, applications, and digital planning methods

Alexander Paolini[a,*], Stefan Kollmannsberger[a], Ernst Rank[a,b]

[a] Chair for Computation in Engineering, Technical University of Munich, Arcisstr. 21, 80333 Munich, Germany
[b] Institute for Advanced Study, Technical University of Munich, Lichtenbergstr. 2a, 85748 Garching, Germany

ARTICLE INFO

Keywords:
Additive manufacturing
Construction
Large scale
Building Information Modeling
Numerical simulation

ABSTRACT

The application of additive manufacturing (AM) in construction has been increasingly studied in recent years. Large robotic arm- and gantry-systems have been created to print building parts using aggregate-based materials, metals, or polymers. Significant benefits of AM are the automation of the production process, a high degree of design freedom, and the resulting potential for optimization. However, the building components and 3D-printing processes need to be modeled appropriately. In this paper, the current state of AM in construction is reviewed. AM processes and systems as well as their application in research and construction projects are presented. Moreover, digital methods for planning 3D-printed building parts and AM processes are described.

1. Introduction

Additive manufacturing (AM) techniques are used in various industries to create physical prototypes as well as end-use parts. In the construction sector, architectural models have been created with these methods for more than a decade. Furthermore, recent years have seen a vast increase in research on printing methods for building components, and first construction projects have been implemented by applying AM processes [1–4]. This development can be attributed to the opportunities AM offers. AM allows building companies to produce geometrically complex structures, to vary materials within a component according to its functions, and to automate the construction process starting from a digital model. These advantages can be exploited if the building components and AM processes are modeled appropriately in the planning phase. To this end, several digital methods for designing printable parts and for planning AM processes have been developed. In addition, file formats to store and exchange the resulting data have emerged.

In the international standard ISO/ASTM 52900 [5], AM is defined as a “process of joining materials to make parts from 3D model data, usually layer upon layer”. It is an alternative to conventional manufacturing processes, in which, for example, material is formed in molds or subtracted by milling. AM processes can be divided into seven categories: material extrusion, material jetting, binder jetting, powder bed fusion, directed energy deposition, vat photopolymerization, and sheet lamination [5]. The systems that implement AM processes have been developed mainly for small-scale applications and factory production. As building components are often large and made outside of a controlled environment, AM systems have been adapted, which has led to several different solutions [1,6]: In many cases, the printing head is moved by a large gantry robot with three degrees of freedom [8–10]. They can be easily controlled and are able to carry heavy loads. Due to their limited motion capabilities, however, they are not exactly well-suited for printing overhangs without support or for working on existing structures. Moreover, they are relatively cumbersome to install and take up much space [11]. Alternatives to gantry solutions are arm-based systems as described in [11–14]. They are more difficult to control and easier to disturb, but have greater freedom of movement and take up less space. By placing a robot arm on a mobile base as shown in Fig. 1, the construction space can be increased and collisions with the structure can be avoided [11]. Further systems that have been investigated are cable suspended platforms [15] and collaborating robots, both terrestrial [16,17] and aerial [18].

The present paper provides an overview of AM processes and systems for the construction industry in Section 2. Here, material-related aspects are highlighted and applications are presented. Moreover, opportunities and challenges of AM in construction are discussed. Section 3 serves to describe digital planning methods for 3D-printed building parts and AM processes.

* Corresponding Author.
E-mail address: alexander.paolini@tum.de (A. Paolini).

https://doi.org/10.1016/j.addma.2019.100894
Received 2 July 2019; Received in revised form 27 September 2019; Accepted 29 September 2019
Available online 09 October 2019

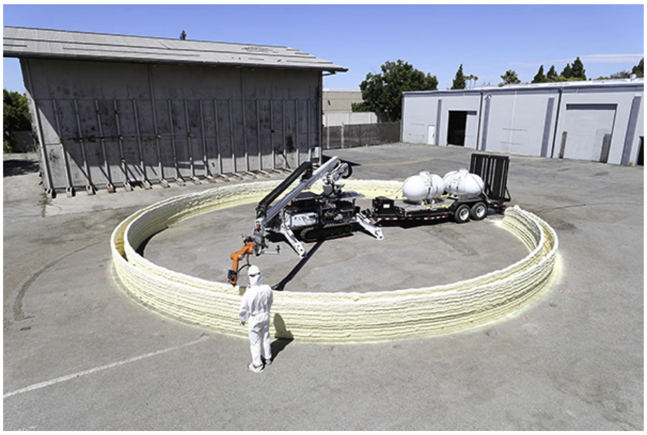

Fig. 1. Digital Construction Platform (DCP) developed at Massachusetts Institute of Technology [7].

2. Processes and applications

AM processes are closely linked to the materials being handled. With regard to the printing of building parts, the research focus has been on aggregate-based materials, metals, and polymers.

2.1. Aggregate-based materials

Aggregate-based materials such as concrete are most common in the field of additive construction. Mainly, material extrusion and particle-bed processes are applied for printing concrete, but other generative approaches such as Smart Dynamic Casting have been studied as well. Since concrete has a relatively low tensile strength and is quite brittle, solutions for the integration of reinforcement have been developed to produce more stable and ductile structures [6,9,10,19–24].

2.1.1. Material extrusion

In concrete extrusion, a structure is created layerwise with a nozzle that deposits fresh cementitious material along a defined path, as exemplarily depicted in Fig. 2. In order to ensure a good quality of the printed components, the material must have certain characteristics: First, it has to be possible to pump the fresh mix to the nozzle. For instance, no particle segregation should occur in the hose to prevent blockages (pumpability) [26–28]. Further, the concrete needs to flow through the nozzle, and the deposited filament should largely retain its shape (extrudability) [26,29]. Also, the new layer has to bond with the underlying one (interlayer adhesion) [26,30–35]. Finally, no significant deformation should occur under the weight of the overlying layers (buildability) [26,27,29,36–39]. To this end, material- and process-related parameters such as the mix proportions and the addition of admixtures as well as the path and speed of the printing head need to be chosen appropriately and matched to each other [26,27,29]. In the hardened state, well printed concrete can have similar strength and density as cast concrete [26]. Measurements shown in [30] demonstrated that an even higher density can be achieved by printing. However, depending on the load direction, the compressive strength of the extruded concrete decreased by up to 15% in the case of straight filaments, and by up to 30% in the case of curved filaments.

Fig. 2. 3D Concrete Printing at Eindhoven University of Technology [25].

Several different concrete extrusion processes were developed in the last years. According to Mechtcherine et al. [19], they can be divided into three types, depending on the filament size:

- **Deposition of fine filaments less than 1 cm in diameter.** An example of this type is 3D Concrete Printing (3DCP) at Loughborough University, for which a 3-axis gantry robot is employed [9,40].
- **Deposition of medium-fine filaments with cross-sectional dimensions up to several cm.** Contour Crafting at University of Southern California [8,41–43] and 3DCP at Eindhoven University of Technology [10,44] belong to this group. In both cases, the printing head is part of a 3-axis gantry robot. Furthermore, in Contour Crafting, trowels are attached to the nozzle in order to achieve smoother and more accurate surfaces.
- **Deposition of coarse filaments in the range of several dm.** CONPrint3D at Technical University of Dresden falls into this category. It strives for an extensive use of established standards for concrete and existing construction equipment. To this end, the modification of an auto concrete pump for printing is being investigated [45].

An advantage of finer filaments is the higher printing resolution, allowing for greater precision and geometric complexity. On the other hand, a filament with larger cross-section leads to higher productivity and enables the use of coarser-grained concrete, resulting in a reduced need for cement and in less shrinkage [19].

In [6], AM systems suitable for concrete extrusion processes are categorized according to the size of the printed object, the layer thickness, the printing environment, the assembling strategy, the use of support structures, and the robotic complexity. It was concluded that 3-axis printing devices are the most common and that mostly layers with a thickness of few cm are produced. Furthermore, only little research on component assembling and support structures was found. Various projects were implemented with these AM systems:

- Loughborough University built a curved bench with the dimensions $2 \times 0.9 \times 0.8\,m^3$ based on its 3DCP concept. The printing took approximately 42 h. The high printing resolution was exploited to create a structured surface and to include individually shaped voids for weight reduction and post placement of reinforcement [9].
- A complex-shaped wall-element measuring $1.36 \times 1.50 \times 0.17\,m^3$ was printed by XtreeE [46] using a 6-axis robot arm. The component is made from ultra-high performance concrete and was geometrically optimized for thermal insulation. The production time was about 12 h [47].
- WinSun [48] printed the components of a single-floored office building with an area of almost $250\,m^2$ for the Dubai Future Foundation. The printing process, which is similar to Contour Crafting, took 17 days. After that, the parts were transported to Dubai and assembled there in 2 days [3,19].
- In the Netherlands, a bicycle bridge with a span of 6.5 m and a width of 3.5 m was constructed by applying 3DCP at the Eindhoven University of Technology. The superstructure of the bridge consists of printed elements, interconnected by subsequently installed tendons. In addition, reinforcement cables were embedded in some layers during their deposition. All elements were printed within 48 h

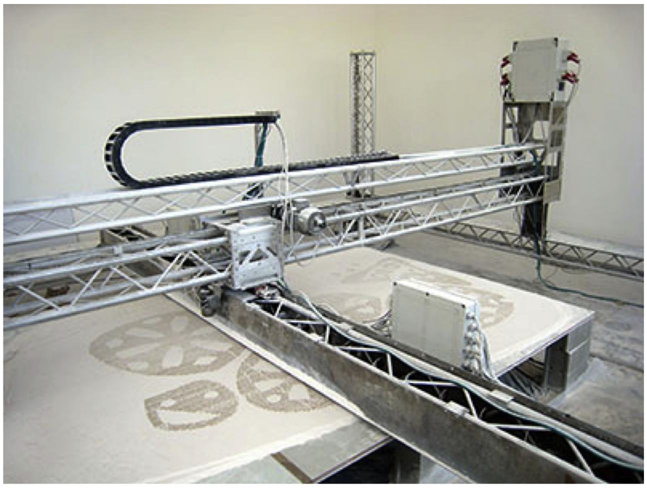

Fig. 3. Cross section produced with a D-Shape printer [55].

[49].

Further projects were carried out by Apis Cor [50], BetAbram [51], CyBe [52], WASP [53], and Total Kustom [54].

2.1.2. Particle-bed processes

Aggregate, binder, and activator such as sand, cement, and water, respectively, are mixed prior to deposition in concrete extrusion processes. By contrast, in particle-bed processes, the raw materials are only brought together on the build platform. Here, a layer of dry particles is first created. Then, a fluid is deposited selectively such that particles are bonded together in certain areas, as can be seen in Fig. 3. This procedure is repeated until all layers are completed, each on top of one another. After that, the printed object is exposed by removing all loose particles, which may be reused. Post-manufacturing processes like infiltration and heat treatment can increase the strength and durability of the printed structure. The construction space is in general more limited than in the case of concrete extrusion processes because it needs to be completely filled with particles. However, particle-bed processes allow for more freedom of design, due to the support from the non-bonded particles. For example, overhangs can be printed without additional support structures. Furthermore, layer thicknesses down to 0.1 mm are possible. Thus, small details can be printed with high accuracy [56].

As defined by Lowke et al. [56], there are three types of particle-bed processes:

- **Selective binder activation.** The particle bed consists of a fine aggregate and binder, for example sand combined with cement. A liquid activator, such as water with admixtures, is added selectively to it.
- **Selective paste intrusion.** The particle bed only contains the aggregate, and the selectively deposited fluid is a binder paste that consists of cement, water, and admixtures.
- **Binder jetting.** The particle bed is a mixture of aggregate and activator. A liquid binder is applied selectively to it. For instance, this method is used to produce sand-molds by locally adding resin on particle beds consisting of sand and hardener.

Particle-bed processes and the properties of the resulting hardened materials, as well as their dependency on material- and process-related parameters, were explored in [57–66]. An overview of these studies is given in [56]. For example, the impact of the water-cement ratio on the strength in the case of selective binder activation was investigated in [61]. The compressive strength reached 16.4 MPa after 7 days. In contrast to conventional production methods, the strength increased with the water-cement ratio. This effect is assumed to be caused by an improved layer bonding and was also observed in [64]. Weger et al. [62,63] showed that the penetration depth of the cement paste has a large influence on the strength in the case of selective paste intrusion. The penetration depth in turn depends on the yield stress of the cement paste and the grain size of the aggregate. In recent studies, compressive strengths of over 70 MPa after 7 days were achieved [56].

An established particle bed system for large-scale applications is D-Shape, developed by Enrico Dini [67]. The D-Shape printer presented in [59] has a 6 m wide printing head with 300 nozzles, controlled by a gantry robot (Fig. 3). As described in [56], a D-Shape printer can now spread particles with a size of 0.2 mm to 4 mm and deposit water, aqueous solutions, or cementitious pastes thereon. Furthermore, binder jet printers for polymer-bound sand molds with large dimensions are produced commercially. For example, the largest printers made by voxeljet [68] have a build volume of $4.0 \times 2.0 \times 1.0\,m^3$ and those by ExOne [69] have a build volume of $2.2 \times 1.2 \times 0.6\,m^3$. Many different concrete structures have been manufactured over the past years by applying particle-bed processes:

- With D-shape printers, more than 1000 parts have been produced since 2008. The first object was the Radiolaria pavilion, which measures $3 \times 3 \times 3\,m^3$ [70]. It was printed as a whole in one week by applying a selective binder activation process. Each particle layer was 5 mm thick and comprised sand and magnesium oxide. The liquid activator was magnesium chloride hexahydrate dissolved in water. Another important example is a pedestrian bridge in Madrid which was made with a D-shape printer in 2016. In this case, a sand-cement mix and water were used [56].
- In the scope of the Bloom project [71], a 2.7 m tall pavilion with a ground area of $3.7 \times 3.7\,m^2$ was built in 2015. It was assembled from 840 customized elements that were printed using cement-containing particle beds [56].
- Sand-molds manufactured with binder jetting processes have been used in several research projects to create complex concrete structures: Züblin, voxeljet, and MEVA Formwork Systems printed the mold for a parabolic concrete column of the new Stuttgart Main Station and tested it successfully off-site [72]. In the Smart Slab project of ETH Zurich, a ceiling consisting of prestressed concrete elements was built for the DFAB HOUSE in Switzerland [73]. The printed formwork was optimized to reduce the material use and to simplify the production process for the concrete elements [56]. Moreover, researchers at ETH Zurich produced and tested topologically optimized slab elements made from printed sand-molds filled with ultra-high performance fiber-reinforced concrete. In contrast to the previous examples, the sand-molds are part of the final structure and were not removed after the concrete casting [74].

2.1.3. FreeFAB, Smart Dynamic Casting and Mesh Mould

Complex temporary formwork adapted to a specific geometry can often be used only once. In order to save waste and costs, the Engineering Excellence Group Sydney studied the production of formwork from recyclable wax employing a 6-axis gantry robot. In their method, which is called FreeFAB, a wax mold is first printed coarsely. Then, its surface is milled to increase the accuracy. After building the concrete part, the wax is melted off and reused [75].

At ETH Zurich, further techniques to generate concrete structures with additive processes have been studied. Smart Dynamic Casting allows to print complex-shaped columns with changing cross-sections. For this purpose, flexible slip formwork is moved along a trajectory by a robot arm while fresh concrete is poured into it. During the process, hydration is monitored with a sensor system to adjust the addition of admixtures and the slipping speed [12,76]. In the Mesh Mould method, an autonomous mobile robot named In-situ Fabricator creates a metal mesh by bending and welding steel wires. The mesh serves as formwork, while the concrete is placed, and as reinforcement, after the concrete has cured [13,77]. Both methods were applied for the construction of the DFAB HOUSE. Smart Dynamic Casting was used to build 3 m high facade mullions with variable cross sections of at least $70 \times 100\,mm^2$. Each mullion could be produced in 4 h [78]. With Mesh Mould, a double-curved, load-bearing wall with a length of 12 m was manufactured [79].

2.1.4. Integration of reinforcement

Several methods have been investigated to reinforce 3D-printed concrete parts in order to improve their structural performance [20,80]. They can be categorized according to whether the reinforcement is external or internal and whether it is installed after, during, or before the concrete deposition:

- **External reinforcement.** With external reinforcement, the printing process does not need to be interrupted and the structure can be assembled from separately printed segments [80]. Two beams with passive external reinforcement, 3 m and 4 m in length, were built and analyzed by Asprone et al. [81]. Further examples are the curved bench made by Loughborough University [9] and the 3D-printed bicycle bridge in the Netherlands [49]. In those cases, prestressed external reinforcement was applied.
- **Internal reinforcement installed within 3D-printed formwork.** Conventional internal reinforcement can be used if regular concrete is poured into a 3D-printed formwork which can be temporary, as described in [72,75], or permanent, as applied by WinSun or ApisCore [80]. Lost formwork made from printed concrete does not have to be considered for load-bearing purposes, but should be taken into account as a concrete cover for the reinforcement to ensure durability. However, the protective effect can be decreased by cold joints between extruded layers. This phenomenon still needs to be investigated in detail [20].
- **Internal reinforcement encased by printed concrete.** Another concept suitable for conventional internal reinforcement is to start off by installing the reinforcement before encasing it with printed concrete. This has been implemented by HuaShang Tengda using a forked nozzle, which, however, limits the height of the pre-installed reinforcement meshes, and by ETH Zurich within its Smart Dynamic Casting method [20,76].
- **Internal reinforcement installed during printing.** Reinforcement parallel to the layer direction can be installed during the printing process. At Eindhoven University of Technology, a method to embed reinforcement cables into the concrete filament was developed and tested with printed beams. Conventional methods to calculate the moment resistance were valid only if a beam failed due to cable breakage. However, in case of cables with high tensile strength, cable slip caused the failures. In order to take advantage of stronger cables, further research on improving the bond with printed concrete is essential [80,82,83].
- **Fiber reinforcement.** The tensile strength and ductility of concrete itself can be increased by adding fibers to the fresh mix [84–88]. A concept to ensure that the fibers cross the joints between extruded layers is being studied at Technical University of Dresden. The idea is to deposit textile strips with vertical fibers in between the layers [20]. Furthermore, as shown in [89–91], cementitious composites with strain hardening behavior have been developed for AM. Most applications, nevertheless, still require reinforcement bars [20].
- **Additively manufactured reinforcement.** For geometrically complex concrete structures, it can be beneficial to manufacture the reinforcement additively like in the Mesh Mould project [13] or in studies performed at the Technical University of Dresden [92]. In the latter investigations, rebars were produced with adequate geometric precision using gas-metal arc welding. However, metal AM is generally much slower than concrete extrusion. For this reason and because of the large heat input during the metal deposition, the reinforcement was not printed at the same time as the concrete. Instead, printable concrete was cast afterwards in order to produce pull-out specimens. In experimental tests, the printed rebars showed about 20% lower yield stress and tensile strength than conventionally produced ones, but they exhibited a larger elongation at break and an approximately equivalent bonding performance [92].

2.2. Metals

In order to print metal parts, powder bed fusion and directed energy deposition processes can be applied. Therein, a heat source such as a laser or an electron beam fuses metal feedstock in the form of powder or wire. Commonly used metals for AM are steels, titanium and its alloys, as well as aluminum alloys. Steels such as 316L austenitic stainless steel or tool steels can be applied for general purposes or parts with higher strength and hardness requirements. Titanium and titanium alloys such as Ti6Al4V are used in particular for high performance parts. Since they are expensive to machine, AM can lead to considerable cost savings. In contrast, aluminum is relatively easy to machine, which is one of the reasons why it is not as thoroughly investigated for use in AM as titanium. 3D-printable aluminum alloys are, for example, AlSi10Mg and AlSi12 [93].

With today's metal AM techniques, it is possible to obtain mechanical properties similar to those resulting from conventional production methods. To this end, a very low porosity is needed [93]. It can be controlled by the quality of the feedstock and the applied volume energy. Both too low and too high energy input can result in voids [94]. Further, the static tensile properties of a printed part strongly depend on its microstructure, which is the result of a complex thermal cycle with repeated heating and cooling processes, due to the addition of overlying layers [93,95]. Because of the higher cooling rate, the microstructures of additively manufactured components are generally finer than those of conventionally produced parts. This leads to higher yield and ultimate strengths [94]. In addition, the microstructure and, hence, the static tensile properties are anisotropic. In most cases, the direction perpendicular to the plane of deposition is the weakest [95]. The fatigue strength can be reduced by material defects like residual porosity and by a coarse surface resulting from the layerwise production process. This problem can be approached with post-manufacturing treatments. The residual porosity can be decreased by heat treatment and hot isostatic pressing, whereas the surface roughness can be reduced by polishing or chemical etching [94]. A more detailed review of the microstructures and mechanical properties of 3D-printed metal parts can be found in [93,95].

Additively and conventionally manufactured building parts made of metal are compared in [96]. One of the components is a small bracket, and the other is a large window frame. It was concluded that it is feasible to produce both components with AM techniques and that the environmental impact can be substantially reduced in this way. On the other hand, production costs and time would be significantly higher if AM processes were applied instead of conventional ones. Potential remedies are, however, mass reductions by optimization, the use of wire feedstock with larger dimensions, and future improvements of metal AM techniques [96]. On the basis of this study, a fast and consistent assessment method was developed to compare the effects of additive and conventional manufacturing for single building components [96]. In the following, metal AM processes and their application to the production of building parts are described.

2.2.1. Powder bed fusion

In powder bed fusion processes such as laser beam melting (LBM), electron beam melting (EBM), and direct metal laser sintering (DMLS), metal powder is first spread across the work area in a closed chamber providing a controlled environment. After that, a laser or an electron beam selectively fuses the powder to create a layer of the final structure. The build platform is then lowered according to the thickness of the layer, and the procedure is repeated until the part is completed

[93]. Powder bed fusion systems typically allow for high geometric accuracy and good mechanical properties, but have a relatively low deposition rate and are mainly used to produce parts with small dimensions such as the following examples [94]:

- A structural node of an existing tensegrity structure was redesigned for AM by Arup. The altered node was produced from stainless steel using DMLS. Its costs were higher than the original node, but it is 75% lighter, which may result in a less expensive overall structure. The new design was derived by means of topology optimization, in which a maximum von Mises stress constraint was enforced to prevent yielding. Several different software applications were used to generate the finite element model, to perform the topology optimization, and to modify the resulting shape in order to obtain a smoother geometry and to take production requirements into consideration. The software programs were well-suited for specific tasks, but there was room for improvement with regard to the interaction between them. Modifications of the geometry after the topology optimization were not automatized and, thus, were rather time consuming. In addition, measurements on 3D-printed test specimens were carried out. The tensile strength and ductility are sufficient and comparable to those resulting from conventional manufacturing methods [97].
- Buchanan et al. [98] studied the structural behavior of 316L stainless steel stub columns produced by DMLS. They are 200 mm tall and have square hollow cross-sections with an outer edge length of 50 mm. The columns have different wall thicknesses varying from 1 to 5 mm. Their ultimate load was measured with compression tests. The results demonstrate that the structural behavior of the additively manufactured stainless steel stub columns is similar to that of conventionally produced ones. Only the ultimate load of the slender column with 1 mm thick walls turned out slightly lower than the range expected for equivalent conventionally produced columns [98].

2.2.2. Directed energy deposition

In directed energy deposition, a melt pool is created on the surface of the printed structure using a laser, an electron beam, or an electric arc. At the same time, metal powder or wire is added to the melt pool in order to generate an additional layer [93]. A laser and metal powder are applied in laser metal deposition (LMD), whereas an electron beam and metal wire are used in wire arc additive manufacturing (WAAM). Directed energy deposition processes are generally faster than powder bed fusion processes and well-suited for the production of large structures. Moreover, they can be used to refurbish existing parts [95].

Large-scale applications of WAAM have been implemented by MX3D. The printer shown in Fig. 4 consists of a gas metal arc welding machine and a 6-axis industrial robot. It can manufacture metal rods which are connected to each other in a self-supporting manner. In this way, large metal structures such as the dragon bench were printed [99,100]. A current project is the additive construction of a 2.5 m wide and 10 m long stainless steel footbridge, which is supposed to be installed in Amsterdam before the end of 2019 [101]. It was designed by Joris Laarman Lab and Arup. Other project partners are, for example, Autodesk, Oerlikon, TU Delft, and the Imperial College London [102].

2.3. Polymers

Common methods for printing polymer products are the vat photopolymerization process of stereolithography (SLA), the material extrusion process of fused deposition modeling (FDM), the powder bed fusion process of selective laser sintering (SLS) and binder jetting processes, which are also known as three-dimensional printing (3DP). Different polymers are suitable for these AM processes: Liquid photopolymers are cured by light in SLA. Thermoplastics such as acrylonitrile butadiene styrene (ABS) and polylactic acid (PLA) are typical materials for FDM. PLA can also be used in 3DP and the thermoplastic Polyamid 12 (PA12) in SLS [94,104].

For the task of producing building components, photopolymers have been cost prohibitive so far [2]. In addition, many printed polymers are not suitable for heavily loaded parts because of their low stiffness and strength. However, polymer composites with improved mechanical properties, such as carbon fiber reinforced ABS (CF-ABS), have been developed and used for AM [4,94,105,106]. Binder jetting techniques in which polymer binder and sand are processed have been applied to produce formwork for concrete structures, as described in Section 2.1.2. In the following, material extrusion and powder bed fusion processes for polymers as well as their utilization for construction purposes are presented.

2.3.1. Material extrusion

A 3D-printing technique called Big Area Additive Manufacturing (BAAM), which is similar to FDM, has been developed at Oak Ridge National Laboratory to produce large polymer components measuring up to $6 \times 2.4 \times 1.8\,m^3$ [106,108]. In the BAAM system depicted in Fig. 5, a single screw extruder is used to heat up a pelletized thermoplastic feedstock and to deposit the melted material along the tool path. With this pellet-based technique, feedstock costs can be reduced by 20 times, and the deposition rate can be increased by 200 times compared to conventional AM systems processing polymer filaments. The tensile strength and stiffness of different BAAM-printed materials such as neat ABS and CF-ABS were studied with measurements. Pure ABS deposited with the BAAM system had almost isotropic material properties, similar to injection molded ABS. BAAM-printed CF-ABS, in contrast, was anisotropic and showed an improved tensile strength and stiffness in deposition direction. Based on these results, it was concluded that BAAM-

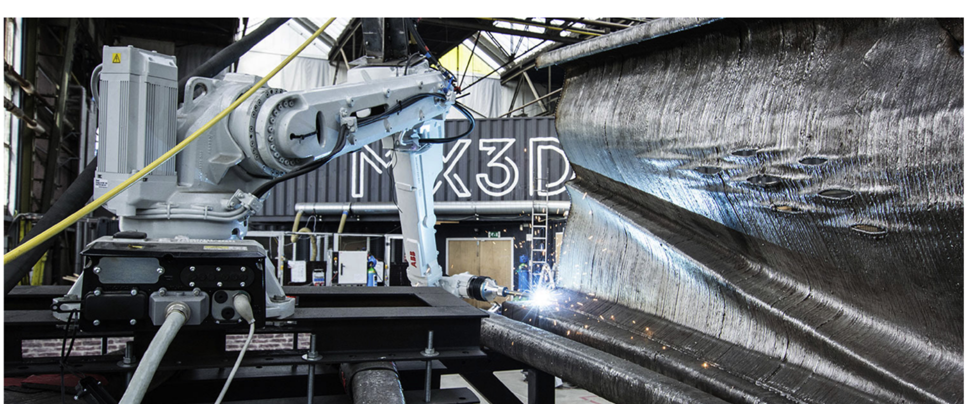

Fig. 4. Metal bridge part manufactured with the MX3D printer [103].

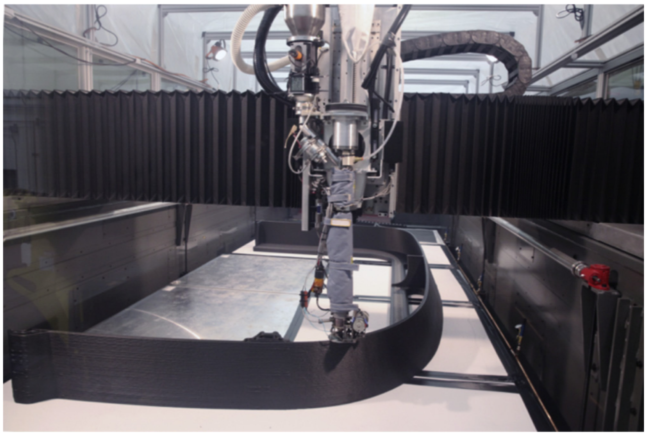

Fig. 5. Building component printed with the BAAM system [107].

deposited materials can be appropriate for certain stiffness-limited applications [106]. The BAAM system was used to print the segments of a cylindrical single-floored building with a ground area of 19.5 m^2 and a height of 2.8 m as part of the research project Additive Manufacturing Integrated Energy (AMIE) [107]. All segments have the shape of a half-ring. Overall, they are made from more than 6 t of CF-ABS and were printed in about 225 h. After that, they were assembled to rings which in turn were joined with four steel rods oriented in longitudinal direction of the building and perpendicular to the printing plane of the segments. Thus, the issue of low tensile strength and stiffness of CF-ABS in build direction was resolved [107].

The Digital Construction Platform (DCP) was created at Massachusetts Institute of Technology. It controls the position of an extrusion nozzle with a 6-DOF electric arm attached to a large 4-DOF hydraulic arm which in turn is mounted on a mobile platform with track rollers, as shown in Fig. 1. Using this printer, a polymeric dome measuring 14.6 m in diameter and 3.7 m in height was built in 13.5 h. Starting from the base, the wall thickness was reduced continuously towards the top. A two-component polyurethane closed cell foam was used as building material. Tests confirmed that this material can also be used to print permanent formwork for concrete, since its average failure pressure is similar to that of commercial insulated concrete formwork [11].

Other examples of large-scale 3D-printers extruding polymers are [3,109]:

- KamerMaker by DUS Architects [110],
- Customized 3D-printers by BLB Industries [111],
- Delta WASP 3MT by WASP [53],
- Large Scale Additive Manufacturing machine by Thermwood [112],
- AiMaker by Ai Build [113],
- C-Fab printer by Branch Technology [114],
- Minibuilders developed at the Institute for Advanced Architecture of Catalonia [17].

2.3.2. *Powder bed fusion*

In the powder bed fusion process SLS, layers of polymer powder are iteratively applied on top of each other, analogous to DMLS. Between each step, a laser selectively heats up the polymer particles of the respective layer such that they are fused together in certain areas without being fully melted. Benefits of SLS are the high resolution and quality which can be achieved. However, it is more expensive and slower than material extrusion processes [94].

SLS was applied by Skanska and 3D Systems in order to produce the geometrically complex polymer cladding for the welded steel nodes of the roof structure that was built on top of the 6 Bevis Marks Building in London. The 3D-printed covering does not have a structural function, but it was added for aesthetics and is resistant to rain, sunlight, and heat [115,116].

2.4. *Opportunities and challenges*

Conventional construction processes such as bricklaying, installation of reinforcement, and concrete casting involve heavy manual labor and are often dangerous. By increasing the degree of automation, AM can reduce physical workload and improve workplace safety [11]. AM could also be used for construction projects in harsh environments, for example in places affected by natural disasters, war zones, or extraterrestrial locations [1]. Therefore, NASA and ESA have been conducting and supporting research on the use of lunar material for additive construction techniques such as Contour Crafting [117,118] and D-Shape [59]. The application of AM processes can, moreover, reduce labor costs. However, even if a smaller workforce and lower material usage are necessary, more expensive raw materials and equipment can lead to higher overall costs [1,2]. Further, the production time can be longer and the part size more limited than in the case of conventional production methods. For this reason, many AM processes and systems have to be improved, but also case studies, databases, and assessment methods, for example as described in [96], are needed to predict the producibility, the manufacturing time and costs, as well as the environmental impact of 3D-printed building parts.

Apart from the aspect of automation, AM offers great freedom of design. By combining and varying the raw materials during the AM process, it is possible to produce objects consisting of functionally graded materials (FGM). Thus, for example, the strength can be increased in strongly loaded areas [1,119]. Furthermore, complex external and internal geometries can be obtained to improve the functionality or appearance of a building part. For instance, voids of different shapes and sizes can be included to add air ducts or wiring conduits. Moreover, lightweight cellular structures with mesoscale features sizing 0.1 to 10 mm or even microscale features smaller than 0.1 mm can be created [120]. They can also be graded and can have extraordinary material properties such as a combination of high stiffness and high vibrational damping [121]. In each step of the layerwise production process, however, it has to be ensured that the printed part is stable and that it does not deform significantly. Hence, support structures might be necessary. Alternatively, the part can be designed in such a way that it is self-supporting during the whole manufacturing process. Another geometry-related constraint resulting from the layerwise approach is the surface roughness. A smaller layer thickness or finishing operations can lead to a higher surface accuracy and smoothness, but also to a longer production time [122].

The high degree of design freedom offers extensive possibilities for optimization. For this purpose and to perform structural verifications, it should be possible to predict the properties of the printed parts accurately. As described above, measurements have already been conducted for various AM processes, but only to a limited extent. Further tests and standardizations are essential to enable engineers to derive reliable product properties depending on the chosen feedstock material, printing process, and process parameters. To this end, it is also necessary to develop and validate simulation models for different AM processes [44]. Moreover, a widely automated digital planning workflow is needed, allowing to represent and store complex geometric and material data, to consider manufacturing constraints, as well as to perform numerical simulations efficiently for any printable geometry.

3. Digital planning methods

3D-printers require specific commands to manufacture parts. The digital workflow for generating these machine instructions starts off by designing the object considering functional and aesthetic aspects. In the case of building components, often, high requirements on the structural performance must be fulfilled. There are different approaches to obtain the geometry and material arrangement of a part. In particular, if its function plays a major role, design and digital modeling should be closely linked to each other. Thus, numerical methods can be applied for form finding and dimensioning. For example, a digital 3D model created manually with feature-based computer-aided design (CAD) software can be modified using size and shape optimization. Alternatively, an object can be designed and modeled right from the beginning in a highly automated manner by means of topology optimization [123]. This method can lead to light weight structures with great performance by exploiting the increased design freedom AM offers. An example is the metal node described in Section 2.2.1. However, aspects such as support structures, minimum length-scales, material anisotropy, and multiple scales need to be considered [124]. After the design phase, the CAD model is converted into a form suitable for planning the AM process. At present, the stereolithography (STL) file format, which only requires a surface triangulation, is most widely used [122]. In the process planning phase, the converted geometric model of the part is positioned and oriented in the build space, supplemented by support structures (if necessary), and sliced. Then, the tool path is generated and the process parameters are selected before they are finally translated to a machine language such as G-Code in order to numerically control the printer [125].

STL files describe AM parts by their surface using planar triangular facets, each of which is represented by three vertices and a normal vector. Because of their simple structure, the files can be easily created and read. However, they are only able to include geometry information and to represent an approximation of the CAD model. They contain redundancies and can be very large, especially when curved surfaces have to be modeled accurately. Furthermore, they are prone to flaws such as gaps, intersections, overlaps, or incorrectly oriented facets. Apart from STL, there are also alternative formats that offer a more detailed and reliable data exchange such as AMF, 3MF, STEP, and IFC [126]. For the construction sector, Industry Foundation Classes (IFC) is generally considered the most promising format in this context because it has the potential to fully integrate the planning workflow for AM into the Building Information Modeling (BIM) method.

3.1. Building Information Modeling

A Building Information Model is a comprehensive digital representation of a building that contains geometric and semantic data such as building element types and material properties. Since this data is interlinked, many planning processes can be automated to a high degree. Examples are quantity assessments, collision checks, as well as the generation of simulation models or construction plans. Furthermore, redundancies and inconsistencies between architects and external specialists can be avoided [127,128]. Thus, BIM can significantly improve the planning quality and efficiency, not only for conventionally but also for additively manufactured building components. However, the integration of AM parts into Building Information Models without design restrictions imposes high demands on the geometric and material representation. Methods to meet these requirements are described in the following. Furthermore, the capabilities of the open BIM standard IFC and its application to AM are shown.

3.1.1. Geometry and material representation

Various techniques have been developed for the representation of geometric and material data [119,129–132]. On their basis, almost any printable part such as a cellular structure or an FGM object can be modeled. The geometry of a solid body can be described by means of the following methods:

- **Boundary representation (B-rep).** With B-rep approaches, a solid is represented by its surface which is explicitly modeled, for example, with polygonal meshes or bivariate NURBS patches [129].
- **Volume representation (V-rep).** V-rep techniques allow for the explicit representation of a solid by its volume using, for example, voxels, polyhedral meshes, trivariate NURBS patches [133,134], Constructive Solid Geometry (CSG), or extensions of CSG [129,135].

The application of these methods to cellular structures was reviewed in [129]. B-rep with polygonal meshes was considered the most suitable solution in the case of homogenous material, due to the low computational and memory costs as well as the high robustness.

In order to model an FGM object, the material composition, meaning the shares of the primary materials, at each point $\boldsymbol{x}$ can be specified by an additional vector $\boldsymbol{m}$ [132]. Furthermore, the material distribution, which is the variation of $\boldsymbol{m}$ along $\boldsymbol{x}$, can be described by extending the geometric model, or by using geometry-independent functions that refer to specific coordinate systems or control features [119]:

- **Geometric-model-based material distribution function.** The material distribution in a V-rep model and on the surface of a B-rep model can be defined with the same functions that are used to represent the geometry. In order to describe the material distribution inside of a B-rep model, distance-based functions can be applied [119]. In the case of CSG, the primitives can be complemented with a material representation and combined with each other using the heterogeneous Boolean operators presented in [136].
- **Coordinate-system-based material distribution function.** Independently from the geometry representation, the material distribution can be defined with respect to a Cartesian, cylindrical, or spherical coordinate system using linear or non-linear, discrete or continuous functions [119].
- **Control-feature-based material distribution function.** Control features are points, curves, or 2D regions with predefined possibly varying material compositions. The material composition at any point in space can be derived from control features and distance-based weighting functions [119,132].

Each of these methods has advantages and disadvantages. On the basis of V-rep, for example, complex FGM objects can be modeled with great accuracy. Despite the possibility for adaptive refinement, however, the computational and memory costs can be high. In contrast, CSG-based representations of FGM objects generally need less memory, but the material definition on the level of the primitives can be inconvenient. If the geometry and material are defined separately, they do not restrict each other, making it easier to create complex designs. Usually, material distribution functions based on control features offer more freedom of design than those referring to a specific coordinate system [119].

In order to ensure the functionality of a part and its compatibility with neighboring components, tolerances for geometric features and material properties should be defined. The National Institute of Standards and Technology (NIST) investigated the extension of geometric dimensioning and tolerancing standards to better match the characteristics of AM. In [137], issues related to the specification of geometric tolerances for printed parts were identified followed by solution proposals. Furthermore, the usage of transition regions for tolerancing material compositions was presented in [138].

3.1.2. Industry Foundation Classes

The IFC data model, which is standardized in ISO 16739 [139], allows for a vendor-neutral exchange of BIM data. Like the data models specified in the STEP application protocols, it is based on the object-oriented data modeling language EXPRESS defined in ISO 10303 [140]. With IFC, several geometry descriptions such as a CSG model and a B-rep model consisting of NURBS surfaces can be related to a building element. It is also possible to define a triangulated model based on a list of points. Moreover, building elements composed of multiple materials can be described as well [127]. However, in the present standardized version, an explicit description of volumetric information in the form of voxel models, polyhedral meshes, or trivariate NURBS patches cannot be directly made with IFC objects. Also, the possibility to represent graded material in IFC files by various types of material distribution functions needs to be developed and implemented.

Despite the significant advantages of integrating BIM with AM systems, it has been studied only scarcely. The lack of research in this field was also noted by Yin et al. [141] in the scope of off-site construction. Strategies to plan the AM process based on BIM data were developed and implemented in [142] and [143]. In both cases, IFC is used for a data transfer from the software application for geometric modeling to that for process planning. Results of the proposed frameworks are shown but only for small-scale examples. Furthermore, it is suggested in [142] to extend Building Information Models by additional parameters describing the print material and construction robot in order to provide data necessary for process planning.

3.2. Structural verification

The structural performance of buildings is one of the most crucial aspects in the construction industry. Unfortunately, the possibilities for real testing are limited due to cost pressure, the unique nature of most buildings, and their large dimensions. Thus, their mechanical behavior must be computationally predicted in many cases. The finite element method (FEM) has proven as very powerful for computing the stresses and deformations of structures with almost any geometric complexity. However, it is essential that the FE model is validated and that it provides reliable and accurate results at acceptable computational costs. Furthermore, it should be possible to generate the model efficiently. The modeling effort, which is especially large in the case of complex geometries and material distributions, can be considerably reduced with advanced computational techniques, for example by employing a fictitious domain approach such as the finite cell method (FCM, Fig. 6) [144,145], by decomposing the domain with the Mortar method [146,147], and by homogenizing heterogeneous structures [148,149].

In the following, FEM-based approaches for the structural verification of AM parts are briefly reviewed. A distinction is made between the printing process and the built-in state. It should be noted that, apart from the simulation of concrete structures, most of the methods have not been developed specifically for construction. Nevertheless, due to their importance also in the field of construction engineering, they are included here.

3.2.1. Verification of AM processes

Models for simulating AM processes are being developed to improve the print quality because failures and large deformations can be prevented by better adapting the part orientation, support structures, and process parameters to the specific conditions of each printing process. Also, distortions can be compensated by changing the input geometry. The process simulation techniques differ depending on the raw material:

- **Aggregate-based materials.** The failure of a concrete structure during printing cannot necessarily be predicted analytically as described in [23,37] since a possible loss of stability is not taken into account. Wolfs et al. [36] thus developed an FE-based method to model fresh prints produced with the concrete extrusion process 3DCP of Eindhoven University of Technology. In this approach, a geometrically non-linear structural mechanical FE model is incrementally extended by element layers. The element layers represent newly deposited concrete using a Mohr-Coulomb material model with age-dependent parameters determined from experiments. In addition, measurements were performed during the printing process and compared to the results of the simulation model. The predicted failure deformation was qualitatively correct, whereas the stability of the structure was overestimated in the FE analysis. As discussed in [36], one reason for this might be the lack of geometric and material imperfections in the simulation. Furthermore, the fresh concrete was compacted in the tests to derive the material parameters, but not in the printing process.
- **Metals.** A roadmap for predicting the material properties, residual stresses, and distortions evolving in metal AM processes due to high temperature gradients is provided in [150]. It covers multiple scales and physical aspects. In this strategy, the temperature field during the AM process is calculated on the macroscale by a thermal analysis based on the non-linear heat diffusion equation. The moving heat source can be modeled with a double-ellipsoidal heat flux distribution, proposed by Goldak [151]. For SLM, an alternative heat source model can be found in [152] and for EBM in [153]. Furthermore, the deposition of material can be considered by successively activating quiet or inactive solid finite elements [150]. On the basis of the temperature field, the thermal strain and material properties such as the yield stress are calculated at each integration point for the subsequent mechanical simulation. The thermal and mechanical analysis are commonly performed with the same mesh and polynomial order. They are both transient and non-linear. Furthermore, the dimensions of the moving heat source are generally much smaller than those of the complete domain. Thus, the computational costs can be high. However, there are ways to improve the efficiency. For example, several time steps can be summarized by imposing an energy-equivalent heat source [154,155], the underlying physical model can be simplified [154], or the spatial discretization can be dynamically refined and coarsened [156–158]. Apart from the macroscopic thermo-mechanical analysis, smaller scale models are presented in [150]. They serve to determine meltpool dimensions, heating and cooling rates, as well as metallurgical properties. These results can be used as input for the calculation of the residual stresses on the macroscale [150]. For validation, simulations of metal AM processes have been compared to measurements such as

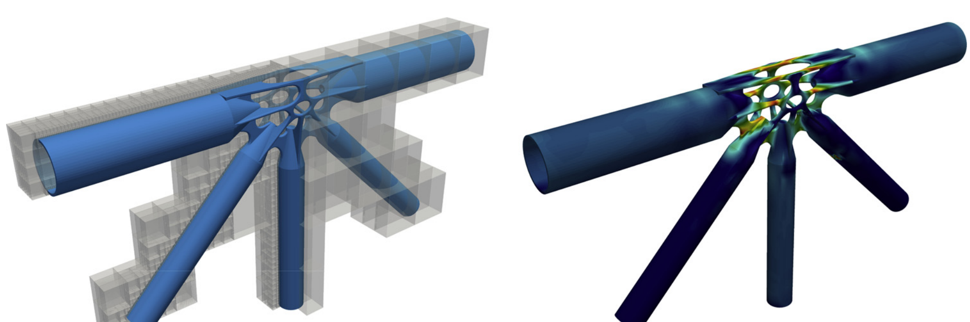

(a) (b)

Fig. 6. FCM model of a steel joint: (a) non-boundary-conforming mesh, (b) computed von Mises stresses. The geometric model was supplied by the Institute of Structural Design at TU Braunschweig.

those of the benchmark test series AM-Bench established by NIST [159–161]. In the cases of stainless steel and tool steels, comparisons of simulations with experiments are presented in [162–165] for powder bed fusion processes and in [166–171] for directed energy deposition processes. However, only partial aspects have been analyzed so far by using calibrated models. There are only few studies, such as those of Megahed et al. [150] and Yan et al. [172], aiming at a comprehensive simulation of metal AM processes by coupling models at multiple scales.

- **Polymers.** Not only for metal but also for polymer AM process simulations, macroscopic thermo-mechanical FE models are used. For material extrusion processes such as SLM and BAAM, process simulation models were presented and validated in [173–176] and for SLS in [177–179]. For example, Brenken et al. [174] measured as a part of their validation work the properties of the print material – a carbon fiber reinforced thermoplastic – and represented it with physics-based models. Thus, the material parameters of the macroscopic FE model did not need to be calibrated. Nevertheless, further research and validations are necessary to simplify the material characterization, to represent different failure mechanisms, and to confirm the results of thermo-mechanical models on larger scales [174].

Apart from the prevention of failures and large distortions during the build process, research on simulation of AM processes strives for the prediction of product properties such as strength and fatigue resistance [172]. The aim is to provide data for the verification of built-in AM parts and to optimize AM processes with regard to the part performance. A major challenge is, however, the development of a comprehensive understanding of the multi-scale and multi-physics mechanisms in AM processes. Further, there is a multitude of interacting factors, the computational costs of detailed simulations are very large, and it is difficult to carry out validations especially at small scales [150,172].

3.2.2. Verification of built-in AM parts

If a building part has a load-transferring function, its stability and serviceability such as the limitation of deformations need to be ensured. Therefore, the respective material and failure behavior in the final state must be known. Experimental data has been used to develop the design and verification procedures for conventionally produced components defined in technical codes such as national standards. For AM parts, such procedures still have to be developed. As described in Section 2, the structural behavior of additively manufactured specimens, which depends on the raw material and the printing process, was experimentally studied and reviewed in [26,30–35] for concrete printing, in [93,98,99] for metal AM, and in [105,106] for polymer extrusion-based AM. In addition, FE models of 3D-printed parts have been created and compared to measurements in [180–183]:

- Crack Mouth Opening Displacement (CMOD) tests on printed concrete with and without fiber reinforcement were simulated numerically at Eindhoven University of Technology. Reasonably accurate results were computed employing a customized constitutive law in tension that had been derived from the CMOD tests. It was proposed to determine the material model from uni-axial tensile tests instead because it may be less ambiguous [180].
- Metal lattice structures made from Ti6Al4V powder were analyzed by Ferrigno et al. [181] and Hedayati et al. [182]. In [181], they were produced by EBM and static tests in tension and compression were conducted. The macroscopic stiffness and strength were derived in each case from the numerical and experimental results for comparison purposes. The investigation showed that a satisfactory agreement with the measurements could only be achieved if the defects were considered in the FE simulations [181]. In [182], SLM was used and fatigue tests were performed. The proposed FEM-based approach to predict the fatigue behavior of porous AM parts led to acceptable results in case the stress level was below 60% of the yield stress. At larger stress levels, the computed life was significantly shorter than the experimentally determined one [182].
- L-shaped polycarbonate rods produced in different orientations using FDM were experimentally tested and simulated by Domingo-Espin et al. [183]. A good agreement between the measurements and FE computations was achieved using orthotropic material parameters that were derived from tensile tests, but also simulations based on averaged isotropic material parameters led to very similar results in the elastic range. However, orthotropic material parameters should be assigned to FDM parts if the yield strength is exceeded [183].

Furthermore, a complex FE model of the MX3D bridge, which is described in Section 2.2.2, was created at Imperial College London to perform geometrically and materially nonlinear analyses. Along with various measurement results, the FE computations are used for the structural verification of the 3D-printed metal bridge [101]. Overall, however, there is a significant lack of experimental data and validated models for printed building components [44,98,184]. This is a major obstacle for establishing computation-based proofs of stability and serviceability.

4. Conclusions

In this paper, the current state of AM in construction was reviewed. Most of the research has been conducted for concrete printing, in particular for concrete extrusion and powder bed processes. Whereas concrete extrusion allows for a larger construction space, powder bed processes offer greater design freedom and higher accuracy. Concrete is widely used in the construction industry because it is easy to process in the fresh state and has a high compressive strength in the hardened state. Moreover, it is compatible with reinforcement steel. For the use in AM, however, it has to be redeveloped. In concrete extrusion, for example, material- and process-related parameters cannot be chosen independently of each other to ensure pumpability, extrudability, interlayer adhesion, and buildability. Additionally, solutions for integrating reinforcement in printed concrete structures have been elaborated. Various projects have been implemented based on this research, for example a bicycle bridge in the Netherlands.

Building components made of metal have been printed with well-developed techniques, for example with the powder bed fusion process DMLS and the directed energy deposition process WAAM. Powder bed fusion enables higher accuracy, while directed energy deposition is generally faster and better suited for large-scale applications such as a stainless steel footbridge.

In order to print building parts from polymers, the most common approach is to employ material extrusion processes. As demonstrated with the BAAM system, the feedstock costs and deposition rate can be vastly reduced by using thermoplastic pellets instead of filaments. For load-bearing purposes, polymer parts can be fiber-reinforced and combined with steel or concrete components. For example, in the project AMIE, a single-floored building was assembled from printed carbon fiber-reinforced ABS components and steel rods.

AM in construction offers considerable freedom of design and extensive possibilities for automation. These benefits can be exploited by using digital planning methods. In this context, the requirements of the construction industry need to be considered. Particularly important is the integration of several different contracting parties already at an early design stage. Therefore, the open BIM standard IFC is increasingly used and demanded in public building projects. IFC has also the potential to fully integrate the planning workflow for AM into the BIM method. However, the IFC standard must be extended to enable a more versatile geometric and material representation as well as to include process planning data. Apart from these conceptual changes, interoperable planning software needs to be developed for different AM systems and tested on large-scale examples.

The design process for buildings also includes extensive structural verifications based on approved rules because the possibilities for experimental testing in a construction project are limited. Thus, another important field of research to advance additive construction is the simulation of AM processes. Numerical methods to model printing processes for concrete, metals, and polymers have been developed and compared with measurements. Their aim is to prevent failures and large deformations during the build process or to predict the product properties. However, only partial aspects have been studied so far. Remaining challenges are, for example, the development of a comprehensive understanding of the multi-scale and multi-physics mechanisms in AM processes and the reduction of the computational costs. Furthermore, in order to verify the stability and serviceability of built-in AM parts, the material and failure behavior must be represented accurately. There is, however, a significant lack of experimental data and validated models for final AM parts.

Conflicts of interest

The authors declare no conflicts of interest.

Acknowledgements

The authors gratefully acknowledge the financial support of the Leonhard Obermeyer Center (LOC).

References

[1] N. Labonnote, A. Rønnquist, B. Manum, P. Rüther, Additive construction: state-of-the-art, challenges and opportunities, Autom. Constr. 72 (2016) 347–366, https://doi.org/10.1016/j.autcon.2016.08.026 ISSN 09265805.

[2] P. Wu, J. Wang, X. Wang, A critical review of the use of 3-D printing in the construction industry, Autom. Constr. 68 (2016) 21–31, https://doi.org/10.1016/j.autcon.2016.04.005 ISSN 09265805.

[3] D. Delgado Camacho, P. Clayton, W.J. O'Brien, C. Seepersad, M. Juenger, R. Ferron, S. Salamone, Applications of additive manufacturing in the construction industry – a forward-looking review, Autom. Constr. 89 (2018) 110–119, https://doi.org/10.1016/j.autcon.2017.12.031 ISSN 09265805.

[4] S.H. Ghaffar, J. Corker, M. Fan, Additive manufacturing technology and its implementation in construction as an eco-innovative solution, Autom. Constr. 93 (2018) 1–11, https://doi.org/10.1016/j.autcon.2018.05.005 ISSN 09265805.

[5] ISO/ASTM 52900.2015, Additive Manufacturing – General Principles – Terminology, International Organization for Standardization, Geneva, Switzerland, 2015.

[6] R. Duballet, O. Baverel, J. Dirrenberger, Classification of building systems for concrete 3D printing, Autom. Constr. 83 (2017) 247–258, https://doi.org/10.1016/j.autcon.2017.08.018 ISSN 09265805.

[7] S.J. Keating, J.C. Leland, L. Cai, B. Darweesh, N. Oxman, Digital Construction Platform, (2017) (accessed: 24.06.19), http://ndagallery.cooperhewitt.org/gallery/66223033/Digital-Construction-Platform.

[8] B. Khoshnevis, Automated construction by contour crafting – related robotics and information technologies, Autom. Constr. 13 (1) (2004) 5–19, https://doi.org/10.1016/j.autcon.2003.08.012 ISSN 09265805.

[9] S. Lim, R.A. Buswell, T.T. Le, S.A. Austin, A.G.F. Gibb, T. Thorpe, Developments in construction-scale additive manufacturing processes, Autom. Constr. 21 (1) (2012) 262–268, https://doi.org/10.1016/j.autcon.2011.06.010 ISSN 09265805.

[10] F. Bos, R. Wolfs, Z. Ahmed, T. Salet, Additive manufacturing of concrete in construction: potentials and challenges of 3D concrete printing, Virtual Phys. Prototyp. 11 (3) (2016) 209–225, https://doi.org/10.1080/17452759.2016.1209867 ISSN 17452759.

[11] S.J. Keating, J.C. Leland, L. Cai, N. Oxman, Toward site-specific and self-sufficient robotic fabrication on architectural scales, Sci. Robot. 2 (5) (2017), https://doi.org/10.1126/scirobotics.aam8986.

[12] E. Lloret Fritschi, L. Reiter, T. Wangler, F. Gramazio, M. Kohler, R.J. Flatt, Smart dynamic casting, slipforming with flexible formwork – inline measurement and control, Proceedings of the 11th High Performance Concrete (11th HPC) and the 2nd Concrete Innovation Conference (2nd CIC), Tromsø, Norway, 2017, https://doi.org/10.3929/ethz-b-000219663.

[13] N. Hack, W.V. Lauer, F. Gramazio, M. Kohler, Mesh mould: robotically fabricated metal meshes as concrete formwork and reinforcement, in: W. Brameshuber (Ed.), Proceedings of the 11th International Symposium on Ferrocement (FERRO-11) and the 3rd International Conference on Textile Reinforced Concrete (3rd ICTRC), RILEM Publications SARL, 2015ISBN 978-2-35158-152-0.

[14] R. Schach, M. Krause, M. Nather, V.N. Nerella, CONPrint3D: 3D-concrete-printing as an alternative for masonry [CONPrint3D: Beton-3D-Druck als Ersatz für den Mauerwerksbau], Bauingenieur 92 (9) (2017) 355–363 ISSN 00056650.

[15] E. Barnett, C. Gosselin, Large-scale 3D printing with a cable-suspended robot, Addit. Manuf. 7 (2015) 27–44, https://doi.org/10.1016/j.addma.2015.05.001 ISSN 22148604.

[16] X. Zhang, M. Li, J.H. Lim, Y. Weng, Y.W.D. Tay, H. Pham, Q.-C. Pham, Large-scale 3D printing by a team of mobile robots, Autom. Constr. 95 (2018) 98–106, https://doi.org/10.1016/j.autcon.2018.08.004 ISSN 09265805.

[17] Institute for Advanced Architecture of Catalonia (IAAC). Minibuilders. http://robots.iaac.net/ (accessed: 24.06.19).

[18] F. Augugliaro, S. Lupashin, M. Hamer, C. Male, M. Hehn, M.W. Mueller, J.S. Willmann, F. Gramazio, M. Kohler, R. D'Andrea, The flight assembled architecture installation: cooperative contruction with flying machines, IEEE Control Syst. 34 (4) (2014) 46–64, https://doi.org/10.1109/MCS.2014.2320359 ISSN 1066033X.

[19] V. Mechtcherine, V.N. Nerella, 3D Printing with concrete: state-of-the art, trends, challenges [3-D-Druck mit Beton: sachstand, entwicklungstendenzen, herausforderungen], Bautechnik 95 (4) (2018) 275–287, https://doi.org/10.1002/bate.201800001 ISSN 09328351.

[20] V. Mechtcherine, V.N. Nerella, Incorporating reinforcement in 3D-printing with concrete [Integration der Bewehrung beim 3D-Druck mit Beton], Beton– und Stahlbetonbau 113 (7) (2018) 496–504, https://doi.org/10.1002/best.201800003 ISSN 00059900.

[21] G.W. Ma, L. Wang, Y. Ju, State-of-the-art of 3D printing technology of cementitious material-an emerging technique for construction, Sci. China Technol. Sci. 61 (4) (2018) 475–495, https://doi.org/10.1007/s11431-016-9077-7 ISSN 16747321.

[22] Y.W.D. Tay, B. Panda, S.C. Paul, N.A. Noor Mohamed, M.J. Tan, K.F. Leong, 3D printing trends in building and construction industry: a review, Virtual Phys. Prototyp. 12 (3) (2017) 261–276, https://doi.org/10.1080/17452759.2017.1326724 ISSN 17452759.

[23] T. Wangler, E. Lloret, L. Reiter, N. Hack, F. Gramazio, M. Kohler, M. Bernhard, B. Dillenburger, J. Buchli, N. Roussel, R. Flatt, Digital concrete: opportunities and challenges, RILEM Tech. Lett. 1 (2016) 67–75, https://doi.org/10.21809/rilemtechlett.2016.16 ISSN 2518-0231.

[24] R.A. Buswell, R.C. Soar, A.G.F. Gibb, A. Thorpe, Freeform construction: mega-scale rapid manufacturing for construction, Autom. Constr. 16 (2) (2007) 224–231, https://doi.org/10.1016/j.autcon.2006.05.002 ISSN 09265805.

[25] Eindhoven University of Technology. 3D Concrete Printing, Photo Gallery. https://www.tue.nl/en/research/research-groups/structural-engineering-and-design/concrete-research-areas/3d-concrete-printing/photo-gallery (accessed: 24.06.19).

[26] R.A. Buswell, W.R. Leal de Silva, S.Z. Jones, J. Dirrenberger, 3D printing using concrete extrusion: a roadmap for research, Cement Concr. Res. 112 (2018) 37–49, https://doi.org/10.1016/j.cemconres.2018.05.006 ISSN 00088846.

[27] T.T. Le, S.A. Austin, S. Lim, R.A. Buswell, A.G.F. Gibb, T. Thorpe, Mix design and fresh properties for high-performance printing concrete, Mater. Struct./Mater. Constr. 45 (8) (2012) 1221–1232, https://doi.org/10.1617/s11527-012-9828-z ISSN 13595997.

[28] V.N. Nerella, V. Mechtcherine, Virtual sliding pipe rheometer for estimating pumpability of concrete, Constr. Build. Mater. 170 (2018) 366–377, https://doi.org/10.1016/j.conbuildmat.2018.03.003 ISSN 09500618.

[29] M. Näther, V.N. Nerella, M. Krause, G. Kunze, V. Mechtcherine, R. Schach, Beton-3D-Druck – Machbarkeitsuntersuchungen zu kontinuierlichen und schalungsfreien Bauverfahren durch 3D-Formung von Frischbeton. Abschlussbericht. Forschungsinitiative Zukunft Bau, Band F 3024, Fraunhofer IRB Verlag, 2017 ISBN 978-3-7388-0028-9. https://www.baufachinformation.de/mobil/forschungsbericht/Beton-3D-Druck-Machbarkeitsuntersuchungen-zu-kontinuierlichen-und-schalungsfreien-Bauverfahren-durch-3D-Formung-von-Frischbeton/248293 (accessed: 24.06.19).

[30] T.T. Le, S.A. Austin, S. Lim, R.A. Buswell, R. Law, A.G.F. Gibb, T. Thorpe, Hardened properties of high-performance printing concrete, Cement Concr. Res. 42 (3) (2012) 558–566, https://doi.org/10.1016/j.cemconres.2011.12.003 ISSN 00088846.

[31] B. Zareiyan, B. Khoshnevis, Interlayer adhesion and strength of structures in contour crafting – effects of aggregate size, extrusion rate, and layer thickness, Autom. Constr. 81 (2017) 112–121, https://doi.org/10.1016/j.autcon.2017.06.013 ISSN 09265805.

[32] B. Zareiyan, B. Khoshnevis, Effects of interlocking on interlayer adhesion and strength of structures in 3D printing of concrete, Autom. Constr. 83 (2017) 212–221, https://doi.org/10.1016/j.autcon.2017.08.019 ISSN 09265805.

[33] B. Zareiyan, B. Khoshnevis, Effects of mixture ingredients on interlayer adhesion of concrete in contour crafting, Rapid Prototyp. J. 24 (3) (2018) 584–592, https://doi.org/10.1108/RPJ-02-2017-0029 ISSN 13552546.

[34] V.N. Nerella, S. Hempel, V. Mechtcherine, Effects of layer-interface properties on mechanical performance of concrete elements produced by extrusion-based 3D-printing, Constr. Build. Mater. 205 (2019) 586–601, https://doi.org/10.1016/j.conbuildmat.2019.01.235 ISSN 09500618.

[35] R.J.M. Wolfs, F.P. Bos, T.A.M. Salet, Hardened properties of 3D printed concrete: the influence of process parameters on interlayer adhesion, Cem. Concr. Res. 119 (2019) 132–140, https://doi.org/10.1016/j.cemconres.2019.02.017 ISSN 00088846.

[36] R.J.M. Wolfs, F.P. Bos, T.A.M. Salet, Early age mechanical behaviour of 3D printed concrete: numerical modelling and experimental testing, Cem. Concr. Res. 106 (2018) 103–116, https://doi.org/10.1016/j.cemconres.2018.02.001 ISSN 00088846.

[37] A. Perrot, D. Rangeard, A. Pierre, Structural built-up of cement-based materials used for 3D-printing extrusion techniques, Mater. Struct./Mater. Constr. 49 (4)

(2016) 1213–1220, https://doi.org/10.1617/s11527-015-0571-0 ISSN 13595997.
[38] N. Roussel, Rheological requirements for printable concretes, Cem. Concr. Res. 112 (2018) 76–85, https://doi.org/10.1016/j.cemconres.2018.04.005 ISSN 00088846.
[39] B. Panda, J.H. Lim, M.J. Tan, Mechanical properties and deformation behaviour of early age concrete in the context of digital construction, Compos. Part B Eng. 165 (2019) 563–571, https://doi.org/10.1016/j.compositesb.2019.02.040 ISSN 13598368.
[40] S. Lim, R. Buswell, T. Le, R. Wackrow, S. Austin, A. Gibb, T. Thorpe, Development of a viable concrete printing process, Proceedings of the 28th International Symposium on Automation and Robotics in Construction, ISARC 2011 (2011) 665–670, https://doi.org/10.22260/ISARC2011/0124.
[41] B. Khoshnevis, R. Dutton, Innovative rapid prototyping process makes large sized, smooth surfaced complex shapes in a wide variety of materials, Mater. Technol. 13 (2) (1998) 53–56, https://doi.org/10.1080/10667857.1998.11752766.
[42] D. Hwang, B. Khoshnevis, An innovative construction process-contour crafting (CC), 22nd International Symposium on Automation and Robotics in Construction, ISARC 2005 (2005).
[43] B. Khoshnevis, D. Hwang, K.-T. Yao, Z. Yeh, Mega-scale fabrication by Contour Crafting, Int. J. Ind. Syst. Eng. 1 (3) (2006) 301–320, https://doi.org/10.1504/IJISE.2006.009791 ISSN 17485037.
[44] T.A.M. Salet, F.P. Bos, R.J.M. Wolfs, Z.Y. Ahmed, 3D concrete printing – a structural engineering perspective, in: M. Lukovic, D.A. Hordijk (Eds.), High Tech Concrete: Where Technology and Engineering Meet – Proceedings of the 2017 fib Symposium, Springer International Publishing, 2017, pp. xliii–lvii ISBN 9783319594705.
[45] R. Schach, M. Krause, M. Nather, V.N. Nerella, CONPrint3D: 3D-concrete-printing as an alternative for masonry [CONPrint3D: Beton-3D-druck als Ersatz für den Mauerwerksbau], Bauingenieur 92 (9) (2017) 355–363 ISSN 00056650.
[46] XtreeE. http://www.xtreee.eu/ (accessed: 24.06.19).
[47] C. Gosselin, R. Duballet, P. Roux, N. Gaudillière, J. Dirrenberger, P. Morel, Large-scale 3D printing of ultra-high performance concrete – a new processing route for architects and builders, Mater. Des. 100 (2016) 102–109, https://doi.org/10.1016/j.matdes.2016.03.097 ISSN 02641275.
[48] Winsun. http://www.winsun3d.com/en (accessed: 24.06.19).
[49] T.A.M. Salet, Z.Y. Ahmed, F.P. Bos, H.L.M. Laagland, Design of a 3D printed concrete bridge by testing, Virtual Phys. Prototyp. 13 (3) (2018) 222–236, https://doi.org/10.1080/17452759.2018.1476064 ISSN 17452759.
[50] Apis Cor. http://apis-cor.com/en (accessed: 24.06.19).
[51] BetAbram. http://betabram.com/ (accessed: 24.06.19).
[52] CyBe. https://cybe.eu/ (accessed: 24.06.19).
[53] WASP. https://www.3dwasp.com/en/ (accessed: 24.06.19).
[54] Total Kustom. http://www.totalkustom.com/ (accessed: 24.06.19).
[55] Edil Tecnico, Tecnologie digitali di stampa 3D: l'applicazione in edilizia, (2016) (accessed: 24.06.19), https://www.ediltecnico.it/37001/tecnologie-digitali-stampa-3d-lapplicazione-in-edilizia/.
[56] D. Lowke, E. Dini, A. Perrot, D. Weger, C. Gehlen, B. Dillenburger, Particle-bed 3D printing in concrete construction – Possibilities and challenges, Cem. Concr. Res. 112 (2018) 50–65, https://doi.org/10.1016/j.cemconres.2018.05.018 ISSN 00088846.
[57] J. Pegna, Exploratory investigation of solid freeform construction, Autom. Constr. 5 (5) (1997) 427–437, https://doi.org/10.1016/S0926-5805(96)00166-5 ISSN 09265805.
[58] G.J. Gibbons, R. Williams, P. Purnell, E. Farahi, 3D Printing of cement composites, Adv. Appl. Ceram. 109 (5) (2010) 287–290, https://doi.org/10.1179/174367509X12472364600878 ISSN 17436753.
[59] G. Cesaretti, E. Dini, X. De Kestelier, V. Colla, L. Pambaguian, Building components for an outpost on the Lunar soil by means of a novel 3D printing technology, Acta Astronaut. 93 (2014) 430–450, https://doi.org/10.1016/j.actaastro.2013.07.034 ISSN 00945765.
[60] A. Fromm, 3-D-Printing zementgebundener Formteile: Grundlagen, Entwicklung und Verwendung. Dissertation, Kassel University Press, Kassel, Germany, 2014.
[61] D. Lowke, D. Weger, K. Henke, D. Talke, S. Winter, C. Gehlen, 3D-Drucken von betonbauteilen durch selektives binden mit calciumsilikatbasierten zementen – erste ergebnisse zu betontechnologischen und verfahrenstechnischen einflüssen, in: H.-M. Ludwig (Ed.), Tagungsband 19. Internationale Baustofftagung (ibausil), F.A. Finger-Institut für Baustoffkunde der Bauhaus-Universität Weimar, 2015.
[62] D. Weger, D. Lowke, C. Gehlen, 3D printing of concrete structures using the selective binding method – effect of concrete technology on contour precision and compressive strength, in: K. Maekawa, J. Yamazaki, A. Kasuga (Eds.), Proceedings of the 11th fib International PhD Symposium in Civil Engineering, FIB 2016, A.A. Balkema Publishers, 2016, pp. 403–410 ISBN 9784990914806.
[63] D. Weger, D. Lowke, C. Gehlen, 3D printing of concrete structures with calcium silicate based cements using the selective cinding method – effects of concrete technology on penetration depth of cement paste, in: B. Middendorf, E. Fehling, J. Thiemicke (Eds.), Proceedings of the 4th International Symposium on Ultra-High Performance Concrete and High Performance Materials (HiPerMat), Kassel, Germany, 2016.
[64] P. Shakor, J. Sanjayan, A. Nazari, S. Nejadi, Modified 3D printed powder to cement-based material and mechanical properties of cement scaffold used in 3D printing, Constr. Build. Mater. 138 (2017) 398–409, https://doi.org/10.1016/j.conbuildmat.2017.02.037 ISSN 09500618.
[65] M. Xia, J. Sanjayan, Method of formulating geopolymer for 3D printing for construction applications, Mater. Des. 110 (2016) 382–390, https://doi.org/10.1016/j.matdes.2016.07.136 ISSN 02641275.
[66] M. Xia, J.G. Sanjayan, Methods of enhancing strength of geopolymer produced from powder-based 3D printing process, Mater. Lett. 227 (2018) 281–283, https://doi.org/10.1016/j.matlet.2018.05.100 ISSN 0167577X.
[67] D-Shape. https://d-shape.com/ (accessed: 24.06.19).
[68] Voxeljet. https://www.voxeljet.com/ (accessed: 24.06.19).
[69] ExOne. https://www.exone.com/ (accessed: 24.06.19).
[70] A. Morgante, Radiolaria pavilion, in: R. Glynn, B. Sheil (Eds.), Fabricate 2011, UCL PRESS, London, United Kingdom, 2017, pp. 231–234, , https://doi.org/10.14324/111.9781787352131.
[71] Rael San Fratello. http://www.rael-sanfratello.com/ (accessed: 24.06.19).
[72] J. Teizer, A. Blickle, T. King, O. Leitzbach, D. Guenther, Large scale 3D printing of complex geometric shapes in construction, ISARC 2016-33rd International Symposium on Automation and Robotics in Construction, International Association for Automation and Robotics in Construction (I.A.A.R.C), 2016, pp. 948–956.
[73] Swiss National Centre of Competence in Research (NCCR) Digital Fabrication. DFAB HOUSE, Smart Slab. http://dfabhouse.ch/smart-slab/ (accessed: 24.06.19).
[74] M.A. Meibodi, M. Bernhard, A. Jipa, B. Dillenburger, The Smart Takes from the Strong, in: A. Menges, B. Sheil, R. Glynn, M. Skavara (Eds.), Fabricate 2017, UCL PRESS, London, United Kingdom, 2017, pp. 210–217, , https://doi.org/10.14324/111.9781787350014.
[75] J.B. Gardiner, S. Janssen, N. Kirchner, A realisation of a construction scale robotic system for 3D printing of complex formwork, ISARC 2016 – 33rd International Symposium on Automation and Robotics in Construction (2016) 515–521, https://doi.org/10.22260/ISARC2016/0062.
[76] E. Lloret, A.R. Shahab, M. Linus, R.J. Flatt, F. Gramazio, M. Kohler, S. Langenberg, Complex concrete structures: merging existing casting techniques with digital fabrication, CAD Comput. Aided Des. 60 (2015) 40–49, https://doi.org/10.1016/j.cad.2014.02.011 ISSN 00104485.
[77] N. Hack, W.V. Lauer, Mesh-mould: robotically fabricated spatial meshes as reinforced concrete formwork, Archit. Des. 84 (3) (2014) 44–53, https://doi.org/10.1002/ad.1753 ISSN 00038504.
[78] Swiss National Centre of Competence in Research (NCCR) Digital Fabrication. DFAB HOUSE, Smart Dynamic Casting. http://dfabhouse.ch/smart-dynamic-casting/ (accessed: 24.06.19).
[79] Swiss National Centre of Competence in Research (NCCR) Digital Fabrication. DFAB HOUSE, Mesh Mould. http://dfabhouse.ch/mesh_mould/ (accessed: 24.06.19).
[80] D. Asprone, C. Menna, F.P. Bos, T.A.M. Salet, J. Mata-Falcón, W. Kaufmann, Rethinking reinforcement for digital fabrication with concrete, Cem. Concr. Res. 112 (2018) 111–121, https://doi.org/10.1016/j.cemconres.2018.05.020 ISSN 00088846.
[81] D. Asprone, F. Auricchio, C. Menna, V. Mercuri, 3D printing of reinforced concrete elements: technology and design approach, Constr. Build. Mater. 165 (2018) 218–231, https://doi.org/10.1016/j.conbuildmat.2018.01.018 ISSN 09500618.
[82] F.P. Bos, Z.Y. Ahmed, E.R. Jutinov, T.A.M. Salet, Experimental exploration of metal cable as reinforcement in 3D printed concrete, Materials 10 (11) (2017), https://doi.org/10.3390/ma10111314 ISSN 19961944.
[83] F.P. Bos, Z.Y. Ahmed, R.J.M. Wolfs, T.A.M. Salet, 3D printing concrete with reinforcement, in: M. Lukovic, D.A. Hordijk (Eds.), High Tech Concrete: Where Technology and Engineering Meet – Proceedings of the 2017 fib Symposium, Springer International Publishing, 2017, pp. 2484–2493, , https://doi.org/10.1007/978-3-319-59471-2_283 ISBN 9783319594705.
[84] M. Hambach, D. Volkmer, Properties of 3D-printed fiber-reinforced Portland cement paste, Cem. Concr. Compos. 79 (2017) 62–70, https://doi.org/10.1016/j.cemconcomp.2017.02.001 ISSN 09589465.
[85] B. Panda, S. Chandra Paul, M. Jen Tan, Anisotropic mechanical performance of 3D printed fiber reinforced sustainable construction material, Mater. Lett. 209 (2017) 146–149, https://doi.org/10.1016/j.matlet.2017.07.123 ISSN 0167577X.
[86] B. Nematollahi, M. Xia, J. Sanjayan, P. Vijay, Effect of type of fiber on inter-layer bond and flexural strengths of extrusion-based 3D printed geopolymer, Advanced Manufacturing and Materials, volume 939 of Materials Science Forum, Trans Tech Publications, 2018, pp. 155–162, https://doi.org/10.4028/www.scientific.net/MSF.939.155.
[87] F.P. Bos, E. Bosco, T.A.M. Salet, Ductility of 3D printed concrete reinforced with short straight steel fibers, Virtual Phys. Prototyp. 14 (2) (2019) 160–174, https://doi.org/10.1080/17452759.2018.1548069 ISSN 17452759.
[88] P. Lauff, O. Fischer, Hochdruck- und -zugfeste betonbauteile durch 3D-druck und gerichtete carbonkurzfasern - herstellung und versuche zum tragverhalten und zur Ermüdung, In tagungsband zum 22, Münchener Massivbau Seminar 5 (2018) 1–58.
[89] D.G. Soltan, V.C. Li, A self-reinforced cementitious composite for building-scale 3D printing, Cem. Concr. Compos. 90 (2018) 1–13, https://doi.org/10.1016/j.cemconcomp.2018.03.017 ISSN 09589465.
[90] H. Ogura, V.N. Nerella, V. Mechtcherine, Developing and testing of strain-hardening cement-based composites (SHCC) in the context of 3D-printing, Materials 11 (8) (2018), https://doi.org/10.3390/ma11081375 ISSN 19961944.
[91] S. Chaves Figueiredo, C. Romero Rodríguez, Z.Y. Ahmed, D.H. Bos, Y. Xu, T.M. Salet, O. Çopuroglu, E. Schlangen, F.P. Bos, An approach to develop printable strain hardening cementitious composites, Mater. Des. 169 (2019), https://doi.org/10.1016/j.matdes.2019.107651 ISSN 02641275.
[92] V. Mechtcherine, J. Grafe, V.N. Nerella, E. Spaniol, M. Hertel, U. Füssel, 3D-printed steel reinforcement for digital concrete construction – manufacture, mechanical properties and bond behaviour, Constr. Build. Mater. 179 (2018) 125–137, https://doi.org/10.1016/j.conbuildmat.2018.05.202 ISSN 09500618.
[93] D. Herzog, V. Seyda, E. Wycisk, C. Emmelmann, Additive manufacturing of metals, Acta Mater. 117 (2016) 371–392, https://doi.org/10.1016/j.actamat.2016.07.019

ISSN 13596454.
[94] T.D. Ngo, A. Kashani, G. Imbalzano, K.T.Q. Nguyen, D. Hui, Additive manufacturing (3D printing): a review of materials, methods, applications and challenges, Compos. Part B Eng. 143 (2018) 172–196, https://doi.org/10.1016/j.compositesb.2018.02.012 ISSN 13598368.
[95] W.E. Frazier, Metal additive manufacturing: a review, J. Mater. Eng. Perform. 23 (6) (2014) 1917–1928, https://doi.org/10.1007/s11665-014-0958-z ISSN 10599495.
[96] N. Mrazovic, M. Baumers, R. Hague, M. Fischer, Guiding building professionals in selecting additive manufacturing technologies to produce building components, Mater. Today Commun. 15 (2018) 199–202, https://doi.org/10.1016/j.mtcomm.2018.02.012 ISSN 23524928.
[97] S. Galjaard, S. Hofman, N. Perry, S. Ren, Optimizing structural building elements in metal by using additive manufacturing, Proc. IASS Annu. Symposia 2015 (2) (2015) 1–12 ISSN 2518-6582. https://www.ingentaconnect.com/content/iass/piass/2015/00002015/00000002/art00016 (accessed: 24.06.19).
[98] C. Buchanan, V.-P. Matilainen, A. Salminen, L. Gardner, Structural performance of additive manufactured metallic material and cross-sections, J. Constr. Steel Res. 136 (2017) 35–48, https://doi.org/10.1016/j.jcsr.2017.05.002 ISSN 0143974X.
[99] S. Joosten, Printing a Stainless Steel Bridge, Master's Thesis, Delft University of Technology, Delft, Netherlands, 2015 (accessed: 24.06.19), http://resolver.tudelft.nl/uuid:b4286867-9c1c-40c1-a738-cf28dd7b6de5.
[100] G.S. van Bolderen, Exploration of Stability of 3D-Printed Steel Members, Master's Thesis, Delft University of Technology, Delft, Netherlands, 2017 (accessed: 24.06.19), http://resolver.tudelft.nl/uuid:cf099386-6a89-44f6-849c-0738177e7ea1.
[101] C. Buchanan, L. Gardner, Metal 3d printing in construction: a review of methods, research, applications, opportunities and challenges, Eng. Struct. 180 (2019) 332–348, https://doi.org/10.1016/j.engstruct.2018.11.045 ISSN 0141-0296.
[102] MX3D. MX3D Bridge. https://mx3d.com/projects/bridge-2/ (accessed: 24.06.19).
[103] MX3D. https://mx3d.com/about/ (accessed: 24.06.19).
[104] S.C. Ligon, R. Liska, J. Stampfl, M. Gurr, R. Mülhaupt, Polymers for 3D printing and customized additive manufacturing, Chem. Rev. 117 (15) (2017) 10212–10290, https://doi.org/10.1021/acs.chemrev.7b00074 ISSN 00092665.
[105] P. Parandoush, D. Lin, A review on additive manufacturing of polymer-fiber composites, Compos. Struct. 182 (2017) 36–53, https://doi.org/10.1016/j.compstruct.2017.08.088 ISSN 02638223.
[106] C.E. Duty, V. Kunc, B. Compton, B. Post, D. Erdman, R. Smith, R. Lind, P. Lloyd, L. Love, Structure and mechanical behavior of big area additive manufacturing (BAAM) materials, Rapid Prototyp. J. 23 (1) (2017) 181–189, https://doi.org/10.1108/RPJ-12-2015-0183 ISSN 13552546.
[107] K. Biswas, J. Rose, L. Eikevik, M. Guerguis, P. Enquist, B. Lee, L. Love, J. Green, R. Jackson, Additive manufacturing integrated energy-enabling innovative solutions for buildings of the future, J. Sol. Energy Eng. Trans. ASME 139 (1) (2017), https://doi.org/10.1115/1.4034980 ISSN 01996231.
[108] B.G. Compton, B.K. Post, C.E. Duty, L. Love, V. Kunc, Thermal analysis of additive manufacturing of large-scale thermoplastic polymer composites, Addit. Manuf. 17 (2017) 77–86, https://doi.org/10.1016/j.addma.2017.07.006 ISSN 22148604.
[109] D. Moreno Nieto, V. Casal López, S.I. Molina, Large-format polymeric pellet-based additive manufacturing for the naval industry, Addit. Manuf. 23 (2018) 79–85, https://doi.org/10.1016/j.addma.2018.07.012 ISSN 22148604.
[110] DUS Architects. KamerMaker. http://3dprintcanalhouse.com/ (accessed: 24.06.19).
[111] BLB Industries. http://blbindustries.se/ (accessed: 24.06.19).
[112] Thermwood. http://www.thermwood.com/ (accessed: 24.06.19).
[113] Ai Build. https://ai-build.com/ (accessed: 24.06.19).
[114] Branch Technology. https://www.branch.technology/ (accessed: 24.06.19).
[115] 3D Systems. 3D Printing Hits New Heights in Architecture. https://www.3dsystems.com/blog/2013/09/3d-printing-hits-new-heights-architecture (accessed: 24.06.19).
[116] Skanska. 3D printing for construction. https://www.skanska.co.uk/about-skanska/innovation-and-digital-engineering/innovation/3d-printing (accessed: 24.06.19).
[117] N.J. Werkheiser, J.E. Edmunson, M.R. Fiske, B. Khoshnevis, On the development of additive construction technologies for application to development of Lunar/Martian surface structures using in-situ materials, AIAA SPACE 2015 Conference and Exposition, American Institute of Aeronautics and Astronautics Inc., AIAA, 2015 ISBN 9781624103346.
[118] B. Khoshnevis, M.P. Bodiford, K.H. Burks, Ed. Ethridge, D. Tucker, W. Kim, H. Toutanji, M.R. Fiske, Lunar contour crafting – a novel technique for ISRU-based habitat development, 43rd AIAA Aerospace Sciences Meeting and Exhibit – Meeting Papers (2005) 7397–7409.
[119] B. Zhang, P. Jaiswal, R. Rai, S. Nelaturi, Additive manufacturing of functionally graded material objects: a review, J. Comput. Inf. Sci. Eng. 18 (4) (2018), https://doi.org/10.1115/1.4039683 ISSN 15309827.
[120] Y. Tang, Y.F. Zhao, A survey of the design methods for additive manufacturing to improve functional performance, Rapid Prototyp. J. 22 (3) (2016) 569–590, https://doi.org/10.1108/RPJ-01-2015-0011 ISSN 13552546.
[121] C.S. Andreasen, E. Andreassen, J.Sø. Jensen, O. Sigmund, On the realization of the bulk modulus bounds for two-phase viscoelastic composites, J. Mech. Phys. Solids 63 (1) (2014) 228–241, https://doi.org/10.1016/j.jmps.2013.09.007 ISSN 00225096.
[122] M.K. Thompson, G. Moroni, T. Vaneker, G. Fadel, R.I. Campbell, I. Gibson, A. Bernard, J. Schulz, P. Graf, B. Ahuja, F. Martina, Design for additive manufacturing: trends, opportunities, considerations, and constraints, CIRP Ann. – Manuf. Technol. 65 (2) (2016) 737–760, https://doi.org/10.1016/j.cirp.2016.05.004 ISSN 00078506.
[123] O. Sigmund, K. Maute, Topology optimization approaches: a comparative review, Struct. Multidiscip. Optim. 48 (6) (2013) 1031–1055, https://doi.org/10.1007/s00158-013-0978-6 ISSN 1615147X.
[124] J. Liu, A.T. Gaynor, S. Chen, Z. Kang, K. Suresh, A. Takezawa, L. Li, J. Kato, J. Tang, C.C.L. Wang, L. Cheng, X. Liang, A.C. To, Current and future trends in topology optimization for additive manufacturing, Struct. Multidiscip. Optim. 57 (6) (2018) 2457–2483, https://doi.org/10.1007/s00158-018-1994-3 ISSN 1615147X.
[125] M. Livesu, S. Ellero, J. Martínez, S. Lefebvre, M. Attene, From 3D models to 3D prints: an overview of the processing pipeline, Comput. Graph. Forum 36 (2) (2017) 537–564, https://doi.org/10.1111/cgf.13147 ISSN 01677055.
[126] R.R. Lipman, J.S. McFarlane, Exploring model-based engineering concepts for additive manufacturing, Proceedings of the 26th Solid Freeform Fabrication Symposium, Austin, TX, 2015.
[127] A. Borrmann, M. König, C. Koch, J. Beetz (Eds.), Building Information Modeling – Technology Foundations and Industry Practice, Springer, Cham, 2018, , https://doi.org/10.1007/978-3-319-92862-3 ISBN 978-3-319-92861-6.
[128] A. Paolini, F. Frischmann, S. Kollmannsberger, A. Rabold, T. Horger, B. Wohlmuth, E. Rank, BIM-based structural dynamic analysis using higher-order volumetric finite elements, Bauingenieur 93 (4) (2018) 160–166 ISSN 00056650.
[129] G. Savio, S. Rosso, R. Meneghello, G. Concheri, Geometric modeling of cellular materials for additive manufacturing in biomedical field: a review, Appl. Bionics Biomech. (2018), https://doi.org/10.1155/2018/1654782 ISSN 11762322.
[130] G. Savio, R. Meneghello, G. Concheri, Geometric modeling of lattice structures for additive manufacturing, Rapid Prototyp. J. 24 (2) (2018) 351–360, https://doi.org/10.1108/RPJ-07-2016-0122 ISSN 13552546.
[131] F. Tamburrino, S. Graziosi, M. Bordegoni, The design process of additively manufactured mesoscale lattice structures: a review, J. Comput. Inf. Sci. Eng. 18 (4) (2018), https://doi.org/10.1115/1.4040131 ISSN 15309827.
[132] X.Y. Kou, S.T. Tan, Heterogeneous object modeling: a review, CAD Comput. Aided Des. 39 (4) (2007) 284–301, https://doi.org/10.1016/j.cad.2006.12.007 ISSN 00104485.
[133] F. Massarwi, G. Elber, A B-spline based framework for volumetric object modeling, CAD Comput. Aid. Des. 78 (2016) 36–47, https://doi.org/10.1016/j.cad.2016.05.003 ISSN 00104485.
[134] T. Dokken, V. Skytt, O. Barrowclough, Trivariate spline representations for computer aided design and additive manufacturing, Comput. Math. Appl. (2018), https://doi.org/10.1016/j.camwa.2018.08.017.
[135] B. Wassermann, S. Kollmannsberger, T. Bog, E. Rank, From geometric design to numerical analysis: a direct approach using the finite cell method on constructive solid geometry, Comput. Math. Appl. 74 (7) (2017) 1703–1726, https://doi.org/10.1016/j.camwa.2017.01.027 ISSN 08981221.
[136] K.-H. Shin, D. Dutta, Constructive representation of heterogeneous objects, J. Comput. Inf. Sci. Eng. 1 (3) (2001) 205–217, https://doi.org/10.1115/1.1403448 ISSN 15309827.
[137] G. Ameta, R. Lipman, S. Moylan, P. Witherell, Investigating the role of geometric dimensioning and tolerancing in additive manufacturing, J. Mech. Des. Trans. ASME 137 (11) (2015), https://doi.org/10.1115/1.4031296 ISSN 10500472.
[138] G. Ameta, P. Witherell, A novel transition region representation for additive manufacturing for graded materials, structures and tolerances, Proceedings of the ASME Design Engineering Technical Conference, vol. 1, American Society of Mechanical Engineers (ASME), 2017, https://doi.org/10.1115/DETC2017-68390 ISBN 9780791858110.
[139] ISO 16739-1:2018, Industry Foundation Classes (IFC) for Data Sharing in the Construction and Facility Management Industries – Part 1: Data Schema, International Organization for Standardization, Geneva, Switzerland, 2018.
[140] ISO 10303-1:1994, Industrial Automation Systems and Integration – Product Data Representation and Exchange – Part 1: Overview and Fundamental Principles, International Organization for Standardization, Geneva, Switzerland, 1994.
[141] X. Yin, H. Liu, Y. Chen, M. Al-Hussein, Building information modelling for off-site construction: review and future directions, Autom. Constr. 101 (2019) 72–91, https://doi.org/10.1016/j.autcon.2019.01.010 ISSN 09265805.
[142] O. Davtalab, A. Kazemian, B. Khoshnevis, Perspectives on a BIM-integrated software platform for robotic construction through contour crafting, Autom. Constr. 89 (2018) 13–23, https://doi.org/10.1016/j.autcon.2018.01.006 ISSN 09265805.
[143] L. Ding, R. Wei, H. Che, Development of a BIM-based automated construction system, in: M. Hajdu, M.J. Skibniewski (Eds.), Procedia Engineering, vol. 85, 2014, pp. 123–131, , https://doi.org/10.1016/j.proeng.2014.10.536 Elsevier Ltd..
[144] J. Parvizian, A. Düster, E. Rank, Finite cell method: h- and p-extension for embedded domain problems in solid mechanics, Comput. Mech. 41 (1) (2007) 121–133, https://doi.org/10.1007/s00466-007-0173-y ISSN 01787675.
[145] A. Düster, E. Rank, B. Szabó, The p-Version of the finite element and finite cell methods, in: E. Stein, R. Borst, T.J.R. Hughes (Eds.), Encyclopedia of Computational Mechanics Second Edition, 2017, pp. 1–35, , https://doi.org/10.1002/9781119176817.ecm2003g ISBN 9781119176817.
[146] F. Ben Belgacem, The Mortar finite element method with lagrange multipliers, Numer. Math. 84 (2) (1999) 173–197, https://doi.org/10.1007/s002119900100 ISSN 0029599X.
[147] B.I. Wohlmuth, Discretization Methods and Iterative Solvers Based on Domain Decomposition, Springer, Berlin, 2001, https://doi.org/10.1007/978-3-642-56767-4 ISBN 978-3-540-41083-6.
[148] M.G.D. Geers, V.G. Kouznetsova, W.A.M. Brekelmans, Multi-scale computational homogenization: trends and challenges, J. Comput. Appl. Math. 234 (7) (2010) 2175–2182, https://doi.org/10.1016/j.cam.2009.08.077 ISSN 03770427.
[149] F. Otero, S. Oller, X. Martinez, Multiscale computational homogenization: review

and proposal of a new enhanced-first-order method, Arch. Comput. Methods Eng. 25 (2) (2018) 479–505, https://doi.org/10.1007/s11831-016-9205-0 ISSN 11343060.
[150] M. Megahed, H.W. Mindt, N. N'Dri, H. Duan, O. Desmaison, Metal additive-manufacturing process and residual stress modeling, Integr. Mater. Manuf. Innov. December (5 (1) (2016) 61–93, https://doi.org/10.1186/s40192-016-0047-2 ISSN 2193-9772.
[151] J. Goldak, A. Chakravarti, M. Bibby, A new finite element model for welding heat sources, Metal. Trans. B 15 (2) (1984) 299–305, https://doi.org/10.1007/BF02667333 ISSN 03602141.
[152] H. Wessels, T. Bode, C. Weißenfels, P. Wriggers, T.I. Zohdi, Investigation of heat source modeling for selective laser melting, Comput. Mech. 63 (5) (2019) 949–970, https://doi.org/10.1007/s00466-018-1631-4 ISSN 01787675.
[153] W. Yan, J. Smith, W. Ge, F. Lin, W.K. Liu, Multiscale modeling of electron beam and substrate interaction: a new heat source model, Comput. Mech. 56 (2) (2015) 265–276, https://doi.org/10.1007/s00466-015-1170-1 ISSN 01787675.
[154] M. Chiumenti, X. Lin, M. Cervera, W. Lei, Y. Zheng, W. Huang, Numerical simulation and experimental calibration of additive manufacturing by blown powder technology. Part I: Thermal Analysis, Rapid Prototyp. J. 23 (2) (2017) 448–463, https://doi.org/10.1108/RPJ-10-2015-0136 ISSN 13552546.
[155] J. Lindwall, A. Malmelöv, A. Lundbäck, L.-E. Lindgren, Efficiency and accuracy in thermal simulation of powder bed fusion of bulk metallic glass, JOM 70 (8) (2018) 1598–1603, https://doi.org/10.1007/s11837-018-2919-8 ISSN 10474838.
[156] E. Neiva, S. Badia, A.F. Martín, M. Chiumenti, A scalable parallel finite element framework for growing geometries. Application to metal additive manufacturing, Int. J. Numer. Methods Eng. (2019) 1–28, https://doi.org/10.1002/nme.6085.
[157] S. Jayanath, A. Achuthan, A computationally efficient finite element framework to simulate additive manufacturing processes, J. Manuf. Sci. Eng. Trans. ASME 140 (4) (2018), https://doi.org/10.1115/1.4039092 ISSN 10871357.
[158] S. Kollmannsberger, A. Özcan, M. Carraturo, N. Zander, E. Rank, A hierarchical computational model for moving thermal loads and phase changes with applications to selective laser melting, Comput. Math. Appl. 75 (5) (2018) 1483–1497, https://doi.org/10.1016/j.camwa.2017.11.014 ISSN 08981221.
[159] National Institute of Standards and Technology (NIST). Additive Manufacturing Benchmark Test Series (AM-Bench). https://www.nist.gov/ambench (accessed: 24.06.19).
[160] Z. Gan, Y. Lian, S.E. Lin, K.K. Jones, W.K. Liu, G.J. Wagner, Benchmark study of thermal behavior, surface topography, and dendritic microstructure in selective laser melting of inconel 625, Integrating Materials and Manufacturing Innovation, (2019), https://doi.org/10.1007/s40192-019-00130-x ISSN 2193-9772.
[161] S. Kollmannsberger, M. Carraturo, A. Reali, F. Auricchio, Accurate prediction of melt pool shapes in laser powder bed fusion by the non-linear temperature equation including phase changes, Integr. Mater. Manuf. Innov. (2019), https://doi.org/10.1007/s40192-019-00132-9 ISSN 2193-9772.
[162] M.F. Zaeh, G. Branner, Investigations on residual stresses and deformations in selective laser melting, Prod. Eng. 4 (1) (2010) 35–45, https://doi.org/10.1007/s11740-009-0192-y ISSN 09446524.
[163] M. Schänzel, D. Shakirov, A. Ilin, V. Ploshikhin, Coupled thermo-mechanical process simulation method for selective laser melting considering phase transformation steels, Comput. Math. Appl. (2019), https://doi.org/10.1016/j.camwa.2019.01.019 ISSN 08981221.
[164] S.M. Tawfik, M.N.A. Nasr, H.A. El Gamal, Finite element modelling for part distortion calculation in selective laser melting, Alex. Eng. J. 58 (1) (2019) 67–74, https://doi.org/10.1016/j.aej.2018.12.010 ISSN 11100168.
[165] M. Yakout, M.A. Elbestawi, S.C. Veldhuis, Density and mechanical properties in selective laser melting of Invar 36 and stainless steel 316L, J. Mater. Process. Technol. 266 (2019) 397–420, https://doi.org/10.1016/j.jmatprotec.2018.11.006 ISSN 09240136.
[166] J. Ding, P. Colegrove, J. Mehnen, S. Ganguly, P.M.S. Almeida, F. Wang, S. Williams, Thermo-mechanical analysis of wire and arc additive layer manufacturing process on large multi-layer parts, Comput. Mater. Sci. 50 (12) (2011) 3315–3322, https://doi.org/10.1016/j.commatsci.2011.06.023 ISSN 09270256.
[167] J. Ding, P. Colegrove, J. Mehnen, S. Williams, F. Wang, P.S. Almeida, A computationally efficient finite element model of wire and arc additive manufacture, Int. J. Adv. Manuf. Technol. 70 (1–4) (2014) 227–236, https://doi.org/10.1007/s00170-013-5261-x ISSN 02683768.
[168] F. Montevecchi, G. Venturini, N. Grossi, A. Scippa, G. Campatelli, Finite Element mesh coarsening for effective distortion prediction in wire arc additive manufacturing, Addit. Manuf. 18 (2017) 145–155, https://doi.org/10.1016/j.addma.2017.10.010 ISSN 22148604.
[169] K.L. Johnson, T.M. Rodgers, O.D. Underwood, J.D. Madison, K.R. Ford, S.R. Whetten, D.J. Dagel, J.E. Bishop, Simulation and experimental comparison of the thermo-mechanical history and 3D microstructure evolution of 304L stainless steel tubes manufactured using LENS, Comput. Mech. 61 (5) (2018) 559–574, https://doi.org/10.1007/s00466-017-1516-y ISSN 01787675.
[170] M. Biegler, B. Graf, M. Rethmeier, Assessing the predictive capability of numerical additive manufacturing simulations via in-situ distortion measurements on a LMD component during build-up, in: M. Schmidt (Ed.), Procedia CIRP, vol. 74, Elsevier B.V., 2018, pp. 158–162, , https://doi.org/10.1016/j.procir.2018.08.069.
[171] Z. Nie, G. Wang, J.D. McGuffin-Cawley, B. Narayanan, S. Zhang, D. Schwam, M. Kottman, Y. Rong, Experimental study and modeling of H13 steel deposition using laser hot-wire additive manufacturing, J. Mater. Process. Technol. 235 (2016) 171–186, https://doi.org/10.1016/j.jmatprotec.2016.04.006 ISSN 09240136.
[172] W. Yan, S. Lin, O.L. Kafka, C. Yu, Z. Liu, Y. Lian, S. Wolff, J. Cao, G.J. Wagner, W.K. Liu, Modeling process-structure-property relationships for additive manufacturing, Front. Mech. Eng. 13 (4) (2018) 482–492, https://doi.org/10.1007/s11465-018-0505-y ISSN 20950233.
[173] M.R. Talagani, S. Dormohammadi, R. Dutton, C. Godines, H. Baid, F. Abdi, V. Kunc, B. Compton, S. Simunovic, C. Duty, L. Love, B. Post, C. Blue, Numerical simulation of big area additive manufacturing (3D printing) of a full size car, SAMPE J. 51 (4) (2015) 27–36 ISSN 00911062.
[174] B. Brenken, E. Barocio, A. Favaloro, V. Kunc, R.B. Pipes, Development and validation of extrusion deposition additive manufacturing process simulations, Addit. Manuf. 25 (2019) 218–226, https://doi.org/10.1016/j.addma.2018.10.041 ISSN 22148604.
[175] A. Cattenone, S. Morganti, G. Alaimo, F. Auricchio, Finite element analysis of additive manufacturing based on fused deposition modeling: distortions prediction and comparison with experimental data, J. Manuf. Sci. Eng. Trans. ASME 141 (1) (2019), https://doi.org/10.1115/1.4041626 ISSN 10871357.
[176] Y. Zhang, Y. Chou, Three-dimensional finite element analysis simulations of the fused deposition modelling process, Proc. Inst. Mech. Eng. Part B J. Eng. Manuf. 220 (10) (2006) 1663–1671, https://doi.org/10.1243/09544054JEM572 ISSN 09544054.
[177] M. Ganci, W. Zhu, G. Buffa, L. Fratini, S. Bo, C. Yan, A macroscale FEM-based approach for selective laser sintering of thermoplastics, Int. J. Adv. Manuf. Technol. 91 (9–12) (2017) 3169–3180, https://doi.org/10.1007/s00170-017-9998-5 ISSN 02683768.
[178] A. Amado, M. Schmid, K. Wegener, Simulation of warpage induced by non-isothermal crystallization of co-polypropylene during the SLS process. AIP Conference Proceedings (2015), https://doi.org/10.1063/1.4918509.
[179] D. Riedlbauer, P. Steinmann, J. Mergheim, Thermomechanical simulation of the selective laser melting process for PA12 including volumetric shrinkage, AIP Conference Proceedings (2015), https://doi.org/10.1063/1.4918512.
[180] F.P. Bos, E. Bosco, T.A.M. Salet, Ductility of 3D printed concrete reinforced with short straight steel fibers, Virtual Phys. Prototyp. (2018) 1–15, https://doi.org/10.1080/17452759.2018.1548069 (Published online: November 19).
[181] A. Ferrigno, F. Di Caprio, R. Borrelli, F. Auricchio, A. Vigliotti, The mechanical strength of Ti-6Al-4V columns with regular octet microstructure manufactured by electron beam melting, Materialia 5 (2019), https://doi.org/10.1016/j.mtla.2019.100232 ISSN 25891529.
[182] R. Hedayati, H. Hosseini-Toudeshky, M. Sadighi, M. Mohammadi-Aghdam, A.A. Zadpoor, Computational prediction of the fatigue behavior of additively manufactured porous metallic biomaterials, Int. J. Fatigue 84 (2016) 67–79, https://doi.org/10.1016/j.ijfatigue.2015.11.017 ISSN 01421123.
[183] M. Domingo-Espin, J.M. Puigoriol-Forcada, A.-A. Garcia-Granada, J. Llumá, S. Borros, G. Reyes, Mechanical property characterization and simulation of fused deposition modeling Polycarbonate parts, Mater. Des. 83 (2015) 670–677, https://doi.org/10.1016/j.matdes.2015.06.074 ISSN 02641275.
[184] M. Ashraf, I. Gibson, M.G. Rashed, Challenges and prospects of 3d printing in structural engineering, Proceedings of the 13th International Conference on Steel, Space and Composite Structures, Perth, Australia, 2018.